Water Air Soil Pollut: Focus (2009) 9:203–211
DOI 10.1007/s11267-009-9206-1

Arsenic Removal from Dilute Solutions by High Surface Area Mesoporous Iron Oxyhydroxide

Dilshad Masih · Yoshimi Seida · Yasuo Izumi

Received: 28 November 2008 / Revised: 7 July 2009 / Accepted: 20 July 2009 / Published online: 30 September 2009

Abstract Mesostructured iron oxyhydroxide (FeO_x) and iron oxyhydroxide–phosphate (FeO_xP) composites were organized using dodecylsulfate surfactant as a template. X-ray diffraction studies depicted a lamellar structure of the product. Ion exchange and solvent extraction methods were employed for the removal of the surfactant. Carboxylate ions exchanged lamellar type mesostructured material reorganized to a wormhole-like mesoporous material when heated under N_2 atmosphere. Surfactant was completely removed by carboxylate ions as observed by the Fourier transform infrared spectra. High surface area acetate-exchanged FeO_x (230 $m^2\ g^{-1}$) was obtained after the surfactant removal from the composite (2.8 $m^2\ g^{-1}$). Surface area of acetate-exchanged FeO_xP was the highest (240 $m^2 g^{-1}$) after the removal of the surfactant. Local structure of iron species of FeO_x was investigated by X-ray absorption fine structure spectroscopy. Further, Fe···Fe bond appeared at 3.21–3.25 Å with coordination number 2–3, showing a high degree of un-saturation of Fe···Fe bonds. As compared with bulk iron oxyhydroxide and iron-intercalated montmorillonite, the mesoporous iron materials were highly effective for arsenic removal from low concentrations of aqueous solutions. Furthermore, mesoporous iron materials were stable in aqueous phase.

Keywords Arsenic removal · Mesoporous · Iron oxyhydroxide

D. Masih (✉)
Global Edge Institute, Tokyo Institute of Technology,
4259-G1-33 Nagatsuta, Midori-ku,
Yokohama 226-8503, Japan
e-mail: masih.d.aa@m.titech.ac.jp

Y. Seida
Department of Environmental Chemistry and Engineering,
Tokyo Institute of Technology,
4259-G1-33 Nagatsuta, Midori-ku,
Yokohama 226-8503, Japan
e-mail: seida.y.aa@m.titech.ac.jp

Y. Izumi
Graduate School of Science, Chiba University,
Yayoi 1-33, Inage-ku,
Chiba 263-8522, Japan
e-mail: yizumi@faculty.chiba-u.jp

1 Introduction

Arsenic contamination of drinking water sources is a major environmental problem around the globe affecting millions of people (Smedley and Kinniburgh 2002; Charlet and Polya 2006). Due to high health hazards, especially the carcinogenic risks from the intake of arsenic-contaminated water, its permissible limit in public water supplies has been reduced from 50 to 10 μg/L (WHO 2001). Arsenic species are prevalent as inorganic forms in the contaminated aquifers. Depending upon environmental conditions, inorganic arsenic exists in water as arsenite and arsenate oxyanions or neutral species. Mobility and bioavailability of arsenic depend

on the particular type of its species, arsenite being the most toxic one. Hydrochemistry of arsenic-enriched aquifers in the calamity-hit Bengal area indicate reducing conditions under which arsenite species should be prevalent in the groundwater (Charlet and Polya 2006; Nath et al. 2008). Besides, considerable amount of inorganic arsenite species has been reported even in the surface waters (Ren et al. 2007).

Iron-based materials have high affinity for arsenic, but removal of the most toxic arsenite species is difficult (Farquhar et al. 2002; Dixit and Hering 2003). Most of the studies on arsenic removal from water deal with arsenate only. Due to high affinity of iron for arsenic, iron compounds have been used even for the cost-effective chemical immobilization of arsenic in contaminated soils (Gemeinhardt et al. 2006). Adsorption is one of the most effective and comparatively simple and economical methods for arsenic removal from aqueous solutions. However, to cope with the new regulations, effective adsorbent materials are required, especially for the removal of arsenite species from the solutions of low concentrations. Iron species intercalated in montmorillonite were effective for oxidative adsorption of arsenic (Izumi et al. 2005; Masih et al. 2005). High affinity and oxidative power of iron-intercalated montmorillonite for the arsenite was observed because of the high extent of un-saturation of Fe···Fe coordination (N=2.5) and their homogeneous distribution (Masih et al. 2007).

Mesostructured iron oxyhydroxides (FeO_x) are reported to have a high degree of un-saturation of Fe···Fe coordination number (Wirnsberger et al. 2001). Synthesis of mesostructured iron materials from iron precursor and surfactant has been reported earlier (Tolbert et al. 1997). But after the removal of the surfactant, it was difficult to maintain the organized framework structure. By employing soft methods for surfactant removal, the degree of Fe···Fe coordinative un-saturation of mesostructured FeO_x was retained and iron contents were also not much different than that of the bulk iron oxyhydroxides (Izumi et al. 2006). As-prepared lamellar material transformed into a wormhole-like mesoporous structure when template was substituted with carboxylate ions followed by heating under N_2 atmosphere. Bruner–Emmett–Teller (BET) surface area and porosity of the materials were controlled by these modifications and mild heat treatments. Amorphous iron (III) phosphate is reported to have good adsorption capacity for heavy metals (Yin et al. 2007). Guo et al. reported the synthesis of high surface area mesoporous iron phosphate with the surfactant sodium dodecylsulfate (Guo et al. 2001). In this study, mesoporous iron oxyhydroxide–phosphate (FeO_xP) analog of FeO_x was prepared to see the effect of framework phosphate in strengthening the framework structure and surface acetate on arsenic removal. The materials were used for the arsenic removal from the aqueous solutions in the concentration range of environmental conditions.

2 Experimental

2.1 Preparation of Adsorbent Materials

Syntheses of mesostructured iron oxyhydroxide (FeO_x) and iron oxyhydroxide–phosphate (FeO_xP) composites were carried out under ambient conditions. For the synthesis of mesostructured FeO_x with iron to surfactant molar ratio of 7:1, 50 mL of 0.10 M ferrous chloride (Wako) was mixed with 10 mL of 0.07 M sodium dodecylsulfate (Wako) followed by dropwise addition of 10 mL of 0.25 M H_2O_2 (Wako) under vigorous stirring. The final reaction mixture was kept on stirring for 1 h and then filtered and washed with deionized water. The obtained yellow powder of mesostructured material is called FeO_x composite. For the synthesis of mesostructured FeO_xP, 2.5 mL of 0.05 M Na_3PO_4 (Wako) was mixed with 50 mL of 0.10 M ferrous chloride followed by the same procedure as described above for the FeO_x composite. The surfactant was removed by solvent extraction with ethanol and ion exchange methods. The composite was mixed with 75 mL of 0.05 M sodium formate, sodium acetate, or sodium propionate solution in ethanol and stirred for 30 min at 290 K. The obtained brown powders are called carboxylate-exchanged FeO_x and FeO_xP. Surfactant was also extracted with ethanol at 290 and 333 K for 10 h. Each of the carboxylate-exchanged or ethanol-washed FeO_x and FeO_xP samples was heated under N_2 flow. The color of the obtained powder was reddish brown.

2.2 Characterization of Adsorbent Materials

X-ray diffraction (XRD) patterns of powder samples were recorded on Multiflex-S diffractometer (Rigaku)

using Cu Kα radiation. N_2 adsorption–desorption isotherms were measured at 77 K on Belsorp-mini (Bel Japan) after pre-treatment at 423 K for 2 h under N_2 flow. Specific surface area was calculated by the BET method. For each type of the International Union of Pure and Applied Chemistry (IUPAC)-classified adsorption–desorption isotherm and hysteresis loop, a specific method is available for the calculation of different parameters. Pore size distribution and pore volume were determined by appropriate *t*-plot (microporous material) and DH-plot (mesoporous materials, synonymous BJH method) methods. Thermogravimetric (TG) and differential thermal analyses (DTA) were performed on DTG-60 (Shimadzu). For the measurement of vibrational spectra, 1.0 wt.% of as-prepared and modified samples and reference materials were mixed very well with KBr (Wako) and pressed into 20-mm-diameter disks. Each disk was prepared from 0.16 g homogeneous mixture. The measurements were carried out under ambient conditions on VALOR-III FTIR (Jasco) equipped with a mercury cadmium telluride detector.

2.3 X-Ray Absorption Fine Structure Studies

For the measurements of X-ray absorption fine structure (XAFS) spectra, FeO_x samples and reference iron materials were mixed well with boron nitride while keeping the Fe K-edge absorption jump value of 1.0. XAFS spectra were measured at beamline 10B of Photon Factory in transmission mode using a Si (311) double crystal monochromator. The rising K-edge energy of the 4-μm Fe metal foil was calibrated at 7,111.20 eV (Bearden 1967). Fe K-edge XAFS data analyses were performed using program XDAP. The Fe–O and Fe···Fe bond distances and coordination numbers were based on crystal structure data for α-Fe_2O_3.

2.4 Arsenic Adsorption Test

Arsenic adsorption tests were performed under batch setup at 290 K in polypropylene tubes. Adsorbent materials (50 mg) were immersed in 20 mL of 0.2–32 mg/L test solutions of arsenite (pH 6.6–7.1) and arsenate (pH 6.3–6.7). The mixtures were shaken at a rate of 130 times per minute on a reciprocating shaker for 12 h. The solid and liquid phase was separated by 0.45 μm cellulose membrane. Arsenic concentration of the liquid phase was quantified by inductively coupled plasma-optical emission spectroscopy measurements.

3 Results and Discussion

3.1 Ordered Framework Structure

XRD patterns measured for the FeO_x composite and its derivative compounds are depicted in Fig. 1. In the small-angle XRD pattern of FeO_x composite, main diffraction peak (001) of ordered framework structure was centered at 2.44° (*d*-spacing of 36.3 Å) followed by the second order diffraction peak (002) at 4.92° depicting a typical lamellar structure. As shown in Fig. 2, the main diffraction peak (001) for FeO_xP composite (2.74°) appeared at higher diffraction angle as compared to FeO_x composite (2.44°) indicating a decrease in the *d*-spacing. Calcination was not effective for the removal of the surfactant, and crystallization to α-Fe_2O_3 started at 573 K before reaching the temperature (>673 K) required for the complete removal of the surfactant. After the surfactant removal and ion exchange with carboxylates, the *d*-spacing decreased to 20.2 Å (acetate) along with a decrease in the regularity of the framework structure of FeO_x. The *d*-spacing of ethanol-washed FeO_x

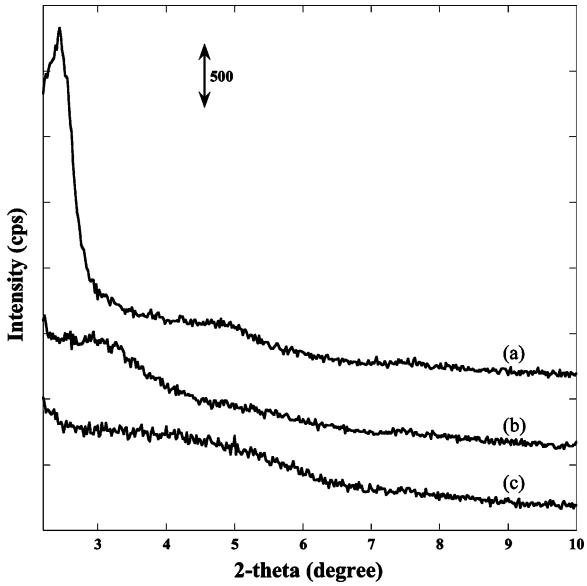

Fig. 1 XRD patterns of FeO_x composite (**a**), ethanol-washed FeO_x (**b**), and acetate-exchanged FeO_x (**c**)

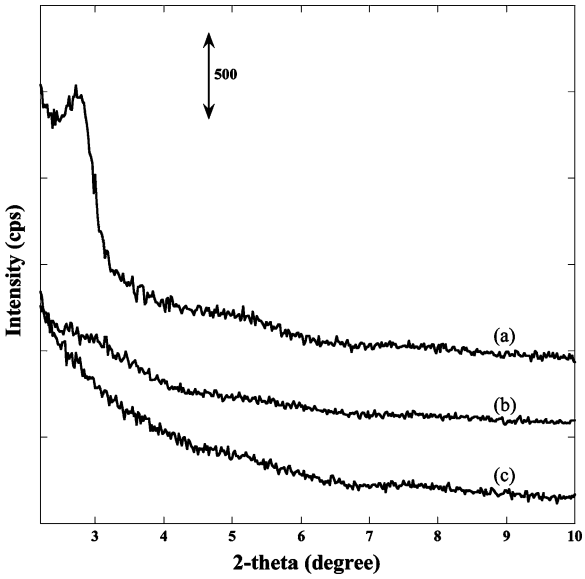

Fig. 2 XRD patterns of FeO_xP composite (**a**), ethanol-washed FeO_xP (**b**), and acetate-exchanged FeO_xP (**c**)

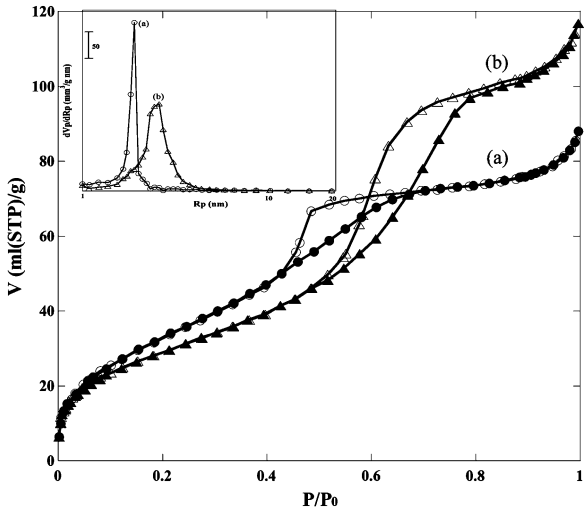

Fig. 3 N_2 adsorption (*solid symbols*)–desorption (*hollow symbols*) isotherms for acetate-exchanged FeO_x (**a**) and propionate-exchanged FeO_x (**b**) materials heated at 533 K (DH-plot is shown in the *inset*)

sample was 28.0 Å. A similar decrease in *d*-spacing and regularity of the framework structure was observed for the FeO_xP material after the removal of the surfactant. Wide-angle XRD patterns in the range of 15–70° showed that the amorphous nature of the as-prepared composites was maintained after the surfactant extraction with ethanol and exchange with carboxylate ions. Small-angle XRD pattern of arsenic adsorbed mesoporous FeO_x showed stability of the framework structure after interaction with aqueous solution. High-resolution transmission electron micrograph of acetate-exchanged FeO_x sample heated at 423 K depicted its prevailing amorphous nature and thin contrast spots of a few nanometers showed a wormhole-like porous nature of the material (Izumi et al. 2006).

3.2 N_2 Adsorption–Desorption Isotherms and Porosity

Type-IVb isotherms of IUPAC classification with characteristic H2-type hysteresis loop were observed for the carboxylate-exchanged FeO_x samples heated at 533 K as shown in Fig. 3 (Rouquerol et al. 1999). Type-IVb isotherms are typical for the wormhole-like mesoporous materials. DH-plot method is appropriate for the calculation of pore size and pore volume from type-IVb isotherms. With DH-plot method, an average pore diameter of 37 Å was determined from desorption branch for the mesoporous material obtained from acetate-exchanged precursor as shown in the inset of Fig. 3. Pore size distribution curve of formate-exchanged FeO_x was also centered at 37 Å. Homogeneous pores of 50 Å was observed for propionate-exchanged FeO_x heated at 533 K (Fig. 3). With the change of the carbon chain length of the carboxylate ions, it was possible to calibrate the pore size for homogeneous mesoporous materials. N_2 adsorption–desorption isotherms measured for three kinds of carboxylate-exchanged FeO_x materials heated at 423 K were of type I. For the type-I isotherms, *t*-plot method is suitable to calculate pore size and pore volume of the materials. From the desorption branch, an average pore size of 10 Å was calculated with *t*-plot method. The isotherm for ethanol-washed sample heated at 423 K belonged to type IV. Figure 4 shows N_2 adsorption–desorption isotherm measured for acetate-exchanged FeO_xP heated at 423 K. The isotherm is typical of wormhole-like mesoporous materials, and pore size was 37 Å as calculated by the DH-plot method, as shown in the inset in Fig. 4. Pore size distribution of acetate-exchanged FeO_xP was also homogeneous.

Other researchers have also reported wormhole-like morphologies of mesoporous iron materials. Srivastava et al. reported the synthesis of mesoporous

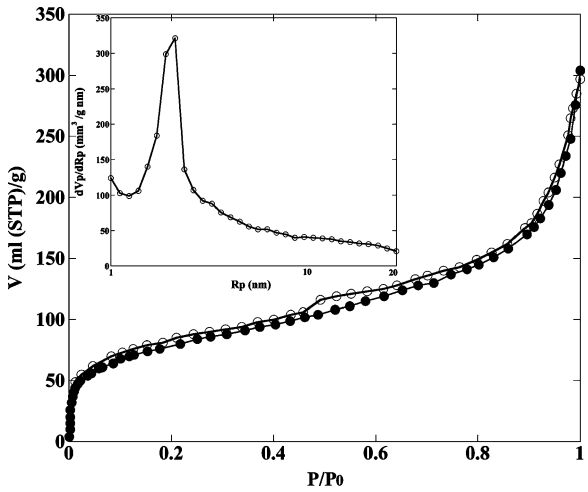

Fig. 4 N_2 adsorption (*solid symbols*)–desorption (*hollow symbols*) isotherms for acetate-exchanged FeO_xP heated at 423 K (DH-plot is shown in the *inset*)

Fe_2O_3 by sonochemical technique, but the product had inhomogeneous pores of 39 and 75 Å (Srivastava et al. 2002). Jiao et al. reported two- and three-dimensional mesoporous Fe_2O_3 with inhomogeneous pore size of 54 and 70 Å (Jiao and Bruce 2004). Mesoporous materials synthesized in this study have homogeneous pores, which is important for the specific application of the materials as adsorbents. An ideal adsorbent material for the removal of arsenic was predicted to have uniform and interlinked pores (Kim et al. 2004). Variations of carboxylate ions were effective to synthesize mesoporous materials with uniform-sized calibrated pores. For the ethanol-washed sample, the pores were also lying in the range of mesopore size (41 Å). However, dV/dR_p peak intensity was by far weaker than the mesoporous materials obtained from the carboxylate-exchanged FeO_x. As-prepared FeO_x composite was essentially non-porous with BET surface area (S_{BET}) of 2.8 $m^2\ g^{-1}$. When surfactant was extracted with ethanol, specific surface area increased to 170 $m^2\ g^{-1}$. Among FeO_x materials, the S_{BET} value was the highest for the acetate-exchanged FeO_x (230 $m^2\ g^{-1}$) material heated at 423 K. It is important to note that, for the acetate-exchanged FeO_x, the S_{BET} value remained high (208 $m^2\ g^{-1}$) even after the interaction with 1.0 mg/L arsenic solution. Pore volumes of mesoporous materials synthesized from propionate-exchanged FeO_x was 0.18 $cm^3\ g^{-1}$. For the mesoporous materials synthesized from formate- and acetate-exchanged FeO_x, the pore volumes were 0.10 and 0.14 $cm^3\ g^{-1}$ respectively. BET surface area of acetate-exchanged FeO_xP was the highest (240 $m^2\ g^{-1}$) among all the mesoporous materials under study. Similar to the highest S_{BET} value, the pore volume of acetate-exchanged FeO_xP was also maximum (0.24 $cm^3\ g^{-1}$) among all the mesoporous materials.

3.3 Thermal Behavior and FT-IR Studies

For the acetate-exchanged FeO_x, a gradual loss of weight was observed between 290 and 500 K as shown by the TG curve in Fig. 5. An early weight loss starting at 330 K was observed because of the desorption of water and acetate species and dehydration of FeO_x. An abrupt weight loss occurred from 500 to 580 K because of the exothermic decomposition of the acetate species as shown by the DTA pattern (Fig. 5). Theoretical weight loss was precisely in agreement with the one observed from the TG curve.

The surfactant, dodecylsulfate, was completely exchanged with carboxylate ions as monitored by Fourier transform infrared (FT-IR) spectroscopy. The spectra measured for FeO_x composite and its derivatives are depicted in Fig. 6. Estimation of the surfactant in the FT-IR spectrum showed that the molar ratio of surfactant and iron in the FeO_x composite was consistent with the starting ratio. When the surfactant was extracted with ethanol, about 25% of the surfactant remained intact as shown by the peak derived from the sulfate (1,227 cm^{-1}) in the

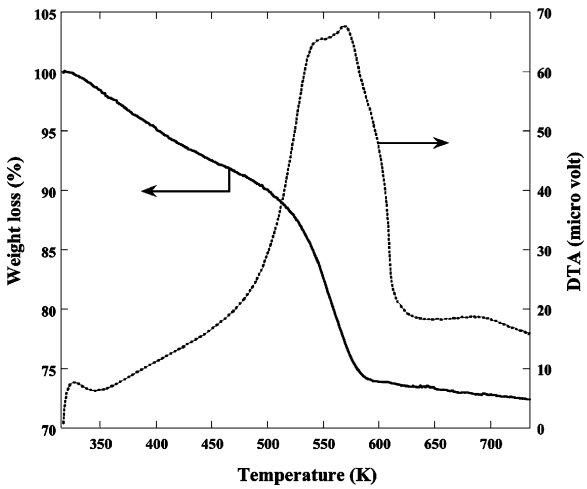

Fig. 5 TG–DTA curves of acetate-exchanged FeO_x

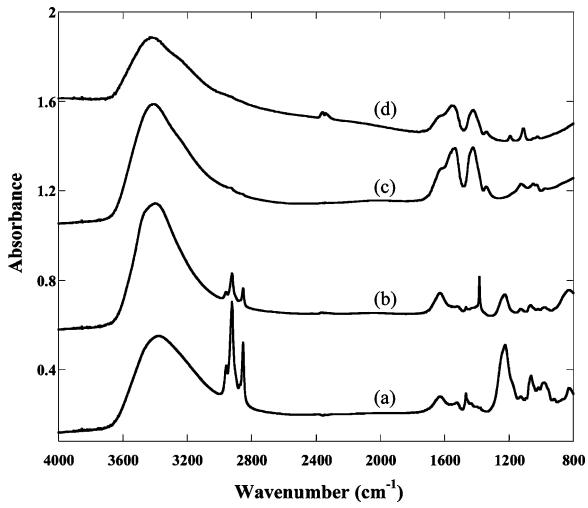

Fig. 6 FT-IR spectra of FeO_x composite (**a**), ethanol-washed FeO_x (**b**), acetate-exchanged FeO_x (**c**), and acetate-exchanged FeO_x heated at 423 K (**d**)

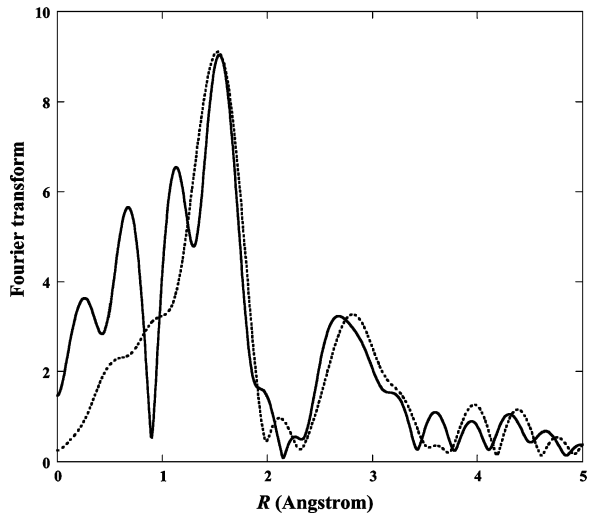

Fig. 7 Fourier transforms of iron K-edge EXAFS spectra measured at 290 K for 14%Fe-montmorillonite (*dotted line*), and acetate-exchanged FeO_x (*solid line*)

FT-IR spectrum (Fig. 6). After surfactant exchange with carboxylates, essentially no dodecylsulfate was detected as depicted by total disappearance of the stretching at 1,227 cm^{-1} due to sulfate. About 51% of the acetate (peaks at 1,423 and 1,540 cm^{-1}) was decomposed on heating at 423 K (Fig. 6).

3.4 Local Structure of Framework Iron Species

Iron K-edge XAFS studies showed a high degree of coordinative un-saturation of Fe···Fe bond in the FeO_x composite and its derivatives. Figure 7 depicts Fourier transforms of extended X-ray absorption fine structure (EXAFS) spectra for FeO_x composite and 14% Fe-montmorillonite. A high degree of coordinative un-saturation has been reported in the 14%Fe-montmorillonite and the material is used as a reference in this study (Izumi et al. 2005). In the Fe K-edge EXAFS Fourier transform, the strongest peak at 1.5–1.6 Å was from Fe–O bond. Another prominent peak at 2.7–2.8 Å was also clearly observed due to Fe···Fe interactions. The Fe–O coordination number negligibly varied around six indicating octahedral [FeO_6] symmetry of iron species. The Fe–O bond distance was 2.05–2.09 Å, relaxed from 2.021 Å for α-FeO(OH) and 2.034 Å for γ-FeO(OH). Accordingly, Fe···Fe bonds were slightly expanded (3.23–3.25 Å) compared to those for the crystalline iron oxides. The Fe···Fe coordination number was in the range of 2–3, similar to that for the 14% Fe-montmorillonite (Fig. 7). As compared to bulk iron oxides, these small values of coordination number indicated a limited number of Fe···Fe attachments and consequently a lot of free sites available to capture arsenic species.

3.5 Arsenic Removal

Arsenic adsorption studies were performed for the removal of arsenite and arsenate species from dilute aqueous solutions in the range of 0.2–32 mg/L. This concentration range is a plausible condition for application to environmental samples. Mesoporous FeO_x, FeO_xP, and reference materials 14%Fe-montmorillonite and α-FeO(OH) were the adsorbent materials used for arsenic removal. Surface area of acetate-exchanged iron oxides was the highest among all the carboxylate-exchanged materials. And preliminary arsenic adsorption tests showed that acetate-exchanged iron oxides were superior in performance. Therefore, results of arsenic removal by acetate-exchanged adsorbents are described in detail. In the applied concentration range, arsenate species was completely removed by the acetate-exchanged FeO_x showing a very high efficiency of the material. Hence, the discussion is focused on the removal of most toxic and difficult-to-remove arsenite species. In Fig. 8, adsorption isotherms are shown for arsenite removal

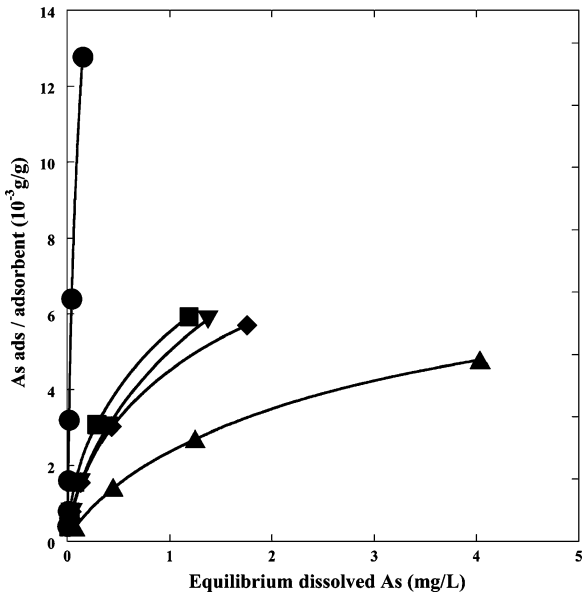

Fig. 8 Adsorption isotherms of arsenite at 290 K on the acetate-exchanged FeO_x (*ball*), ethanol-washed FeO_x (*cube*), acetate-exchanged FeO_xP (*inverted triangle*), 14% Fe-montmorillonite (*diamond*), and ethanol-washed FeO_xP (*triangle*)

from 0.2–32 mg/L solutions. The order of adsorption capacity was mainly depending upon the arsenic concentration at equilibrium. When it was lower than 760 μg/L, the weight ratio of adsorbed arsenic and adsorbent was greatest for the acetate-exchanged FeO_x. Adsorption capacity of bulk material (α-FeO(OH)) employed in this study was far below than that of the acetate-exchanged FeO_x. The acetate-exchanged FeO_x showed much higher adsorption capacity even against the bulk iron oxyhydroxide with the best performance as reported by other researchers (Dixit and Hering 2003). Next, when the concentration was higher than 1.27 mg/L, again the acetate-exchanged FeO_x was matchless in performance. Performance of ethanol-washed FeO_x and 14%Fe-montmorillonite was comparable for arsenite removal from test solution of >1.27 mg/L. Arsenite removal behavior of modified FeO_xP materials was similar to that of modified FeO_x materials. Acetate-exchanged FeO_xP material showed better performance than the ethanol-washed FeO_xP sample.

The difference of arsenic removal efficiencies was mainly due to the order of equilibrium adsorption constant (ml g_{As}^{-1}): 1.0×10^7 (acetate-exchanged FeO_x) $\gg 1.4\times10^6$ (14%Fe-montmorillonite) $> 6.2\times10^5$ (ethanol-washed FeO_x) $\approx 5.4\times10^5$ (α-FeO(OH)), based on the fits with Langmuir-type equation. Thus, the practical superiority of the acetate-exchanged FeO_x is evident. Arsenic uptake of iron oxyhydroxides has been correlated to the adjacent apexes of edge-sharing [FeO_6] units. In the arsenite concentration range studied here, sorption capacity of acetate-exchanged FeO_x heated at 423 K was the greatest. Both the saturated adsorption amount (21×10^{-3} g_{As} $g_{adsorbent}^{-1}$) and adsorption equilibrium constant values were by far greater than ethanol-washed FeO_x, modified FeO_xP, 14%Fe-montmorillonite, and bulk α-FeO(OH) (Izumi et al. 2005; Dixit and Hering 2003).

Arsenic to iron molar ratio for arsenite adsorbed on the acetate-exchanged FeO_x was 15 times higher than that of the bulk α-FeO(OH) employed under the same experimental conditions. High arsenic to iron molar ratio depicts that a large number of adsorption active sites are available in the mesoporous material. Arsenic to iron molar ratio of acetate-exchanged FeO_x was two times greater in comparison to the performance of a high surface area bulk α-FeO(OH) used in another study (Dixit and Hering 2003), even though iron contents of acetate-exchanged FeO_x was 12% less than that of the bulk α-FeO(OH). Furthermore, the As/M (Fe, Al) molar ratio for the arsenite adsorbed on the acetate-exchanged FeO_x was similar to the value reported for mesoporous aluminum oxide (Kim et al. 2004). Iwamoto et al. reported effective removal of arsenate (pH 7.5) and arsenite (pH 10.0) through anion exchange on zirconium sulfate–surfactant micelle mesostructure (Iwamoto et al. 2002). From 5.0 mg/L test solution, almost complete removal of arsenate was observed with the ion exchange time of 10 h. But arsenite removal efficiency of the material was always less than 80% even after 40 h equilibrium time. For the test solutions of similar concentration, acetate-exchanged FeO_x showed complete removal of arsenate and importantly the arsenite removal efficiency was also >99%. High removal efficiency along with high capacity of the adsorbent material is important regarding the modern regulations of arsenic contaminant level, and acetate-exchanged FeO_x was fulfilling the criteria.

The extent of coordinative un-saturation of Fe···Fe bond in the acetate-exchanged FeO_x (N=2.5) and ethanol-washed FeO_x (N=2.6) was similar. The BET specific surface area of the former was 1.35 times larger. These differences were not so remarkable to

justify the extremely good performance of acetate-exchanged FeO_x. Results of Yoshitake et al. showed the importance of creating particular adsorption sites of amino-functionalized mesoporous silica for the arsenate removal but not the surface area (Yoshitake et al. 2002). Also in this study, acetate-exchanged FeO_xP had the highest surface area not the efficiency for arsenite removal. Arsenite exchange against the surface carboxylate species was one of the plausible explanations for the greatest performance of acetate-exchanged FeO_x. However, this cannot explain completely the exceptional performance, as the arsenite species were essentially neutral in the applied pH range of the test solutions. Oxidative adsorption of arsenite on the acetate-exchanged FeO_x could be a possible reason of its extremely high efficiency. Performance of acetate-exchanged FeO_x and FeO_xP was better than the respective ethanol-washed materials. So the porous framework with the presence of adsorbed acetate may be kinetically advantageous over the bare surface mesoporous material.

XRD and BET studies gave valuable information regarding the repeated use of the mesoporous adsorbents. Small-angle XRD pattern showed similar *d*-spacing and extent of the ordered structure before and after arsenic adsorption test. Similar *d*-spacing of mesoporous adsorbent before and after arsenic adsorption is no surprise as the smaller arsenic species fit in the larger vacant area without propping up the iron oxide sheets. Furthermore, the S_{BET} value of acetate-exchanged FeO_x (230 $m^2 g^{-1}$) decreased to 208 $m^2 g^{-1}$ after interaction with 1.0 mg/L arsenic solution. These investigations show stability of the mesoporous iron materials for repeated arsenic removal from aqueous solutions.

4 Conclusions

Surfactant extraction and ion exchange methods were successfully applied to modify mesostructured FeO_x and FeO_xP composites for the efficient arsenic and particularly arsenite removal from low concentrations of test solutions. The lamellar structure of as-prepared composites reorganized to a wormhole-like mesoporous structure. Amorphous nature of the composites was retained after modifications with ethanol and carboxylate solutions of ethanol. Maximum surface area of 230 and 240 $m^2\ g^{-1}$ were obtained respectively for the acetate-exchanged FeO_x and FeO_xP. Carboxylate-exchanged FeO_x heated at 533 K showed wormhole-like homogeneous mesopores of 37 Å (formate/acetate) and 50 Å (propionate). Acetate-exchanged FeO_xP also showed wormhole-like homogeneous-sized pores of 37 Å and maximum pore volume of 0.24 $cm^3\ g^{-1}$. From XAFS studies, Fe···Fe coordination number obtained in the range of 2–3 showed a high degree of coordinative un-saturation of iron species. Acetate-exchanged FeO_x pre-heated at 423 K exhibited the best arsenite sorption capacity and complete removal of arsenate. Adsorbed acetate species in the homogeneous-sized mesoporous network of high surface area acetate-exchanged FeO_x and FeO_xP materials were influencing the high arsenic removal efficiency of the materials.

Acknowledgements XAFS experiments were carried out under the approval of the Proposal Review Committee of Photon Factory. Thanks are due to the Japanese Ministry of Education, Culture, Sports, Science and Technology for the financial assistance from MEXT's program "Promotion of Environmental Improvement for Independence of Young Researchers" under the Special Coordination Funds for Promoting Science and Technology.

References

Bearden, J. A. (1967). X-ray wavelengths. *Reviews of Modern Physics, 39*, 78–124.

Charlet, L., & Polya, D. A. (2006). Arsenic in shallow, reducing groundwaters in Southern Asia: An environmental health disaster. *Elements, 2*, 91–96.

Dixit, S., & Hering, J. (2003). Comparison of arsenic (V) and arsenic (III) sorption onto iron oxide minerals: Implications for arsenic mobility. *Environmental Science & Technology, 37*, 4182–4189.

Farquhar, M. L., Charnock, J. M., Livens, F. R., & Vaughan, D. J. (2002). Mechanism of arsenic uptake from aqueous solution by interaction with goethite, lepidocrocite, mackinawaite, and pyrite: An X-ray absorption spectroscopy study. *Environmental Science & Technology, 36*, 1757–1762.

Gemeinhardt, C., Muller, S., Weigand, H., & Marb, C. (2006). Chemical immobilisation of arsenic in contaminated soils using iron (II) sulfate—advantages and pitfalls. *Water, Air and Soil Pollution: Focus, 6*, 281–297.

Guo, X., Ding, W., Wang, X., & Yan, Q. (2001). Synthesis of a novel mesoporous iron phosphate. *Chemical Communications*, 709–710.

Iwamoto, M., Kitagawa, H., & Watanabe, Y. (2002). Highly effective removal of arsenate and arsenite ion through ion exchange on zirconium sulfate-surfactant micelle mesostructure. *Chemistry Letters, 31*, 814–815.

Izumi, Y., Masih, D., Aika, K., & Seida, Y. (2005). Characterization of intercalated iron (III) nanoparticles and oxidative adsorption of arsenite on them monitored by X-ray absorption fine structure combined with fluorescence spectrometry. *Journal of Physical Chemistry B, 109*, 3227–3232.

Izumi, Y., Masih, D., Aika, K., & Seida, Y. (2006). Creation of micro and mesoporous Fe^{III} materials utilizing organic template followed by carboxylates exchange for the low concentration of arsenite removal. *Microporous and Mesoporous Materials, 94*, 243–253.

Jiao, F., & Bruce, P. G. (2004). Two- and three-dimensional mesoporous iron oxide with microporous walls. *Angewandte Chemie, 116*, 6084–6087.

Kim, Y., Kim, C., Choi, I., Rengaraj, S., & Yi, J. (2004). Arsenic removal using mesoporous alumina prepared via a templating method. *Environmental Science & Technology, 38*, 924–931.

Masih, D., Aika, K., Izumi, Y., & Seida, Y. (2005). Arsenic speciation and identification of active iron adsorbent sites by XAFS spectroscopy. *Proceedings of Environmental Science and Technology, 2*, 435–440.

Masih, D., Izumi, Y., Aika, K., & Seida, Y. (2007). Optimization of an iron intercalated montmorillonite preparation for the removal of arsenic at low concentrations. *Engineering in Life Sciences, 7*, 52–60.

Nath, B., Sahu, S. J., Jana, J., Goswami, A. M., Roy, S., Sarkar, M. J., et al. (2008). Hydrochemistry of arsenic-enriched aquifers from rural West Bengal, India: A study of arsenic exposure and mitigation option. *Water, Air and Soil Pollution, 190*, 95–113.

Ren, J. L., Zhang, J., Li, D. D., Cheng, Y., & Liu, S. M. (2007). Speciation and seasonal variation of dissolved inorganic arsenic in Jiaozhou Bay, North China. *Water, Air and Soil Pollution: Focus, 7*, 655–671.

Rouquerol, F., Rouquerol, J., & Sing, K. S. W. (1999). *Adsorption by powders and porous solids—Principles, methodology, and applications*. London: Academic.

Smedley, P. L., & Kinniburgh, D. G. (2002). A review of the source, behavior and distribution of arsenic in natural waters. *Applied Geochemistry, 17*, 517–568.

Srivastava, D. N., Perkas, N., Gedanken, A., & Felner, I. (2002). Sonochemical synthesis of mesoporous iron oxide and its magnetism and catalytic properties. *Journal of Physical Chemistry B, 106*, 1878–1883.

Tolbert, S. H., Sieger, P., Stucky, G. D., Aubin, S. M., Wu, C., & Hendrickson, D. N. (1997). Control of inorganic layer thickness in self-assembled iron oxide/surfactant composites. *Journal of the American Chemical Society, 119*, 8652–8661.

WHO. (2001). *Guideline for drinking water quality* (3rd ed., vol. 1). Geneva, Switzerland.

Wirnsberger, G., Gatterer, K., Fritzer, H. P., Grogger, W., Pillep, B., Behrens, P., et al. (2001). Mesostructured iron oxyhydroxides. 1. Synthesis, local structure, and magnetism. *Chemistry of Materials, 13*, 1453–1466.

Yin, P., Hu, Y., Sun, Y., Yang, Y., Ji, C., Xu, Q., et al. (2007). Solid-state synthesis of amorphous iron (III) phosphate at room temperature and its adsorption for Hg (II) and Ag (I) ions. *Materials Letters, 61*, 3755–3757.

Yoshitake, H., Yokoi, T., & Tatsumi, T. (2002). Adsorption of chromate and arsenate by amino-functionalized MCM-41 and SBA-15. *Chemistry of Materials, 14*, 4603–4610.